Tunable grating-assisted surface plasmon resonance by use of nano-polymer dispersed liquid crystal electro-optical material

S. Massenot [a,*], R. Chevallier [a], J.-L. de Bougrenet de la Tocnaye [a], O. Parriaux [b]

[a] *Département d'optique UMR CNRS 6082 Foton, GET/ENST Bretagne, Technopole Brest Iroise, CS 83818, 29238 Brest Cedex 3, France*
[b] *Laboratoire Hubert Curien UMR CNRS 5516 (formerly TSI), Université de Saint-Etienne, 18 rue B. Lauras, 42000 Saint-Etienne, France*

Abstract

This paper reports on the experimental observation of the displacement of a surface plasmon resonance (SPR) excited by a metallic diffraction grating. This effect is achieved by the use of an electro-optical material composed of nano-sized droplets of liquid crystals dispersed in a host polymer. The average refractive index of this material in the form of a thin film on the undulated metal surface can be modified with the application of an external electric field and to tune the wavelength at which the SPR excitation leads to a reflection minimum. The theoretical design and experimental demonstration of the principle of this component are described.

Keywords: Surface plasmon resonance; Surface relief grating; Polymer dispersed liquid crystals

1. Introduction

A surface plasmon is a wave propagating along a metallic surface resulting from a collective oscillation of free electrons of the metal. It is a well-known phenomenon extensively used in biology where it allows the real-time monitoring of chemical or biological reactions [1]. Surface plasmons can be excited with TM polarized light either by means of a prism or a diffraction grating coupling configurations [2]. More recently, much research work has been devoted to the study of miniaturized photonic circuits using surface plasmons opening a new domain of physics: Plasmonics (see [3] for example).

Generally, applications using surface plasmon resonances (SPR) are static and the coupling conditions are imposed by the geometry of the setup. Since the propagation constant of a SPR depends on the refractive index of the material placed on the metal surface, as used in biosensors, surface plasmons interestingly lend themselves to a variation of the synchronism coupling condition at fixed incidence angle by means of a modulation of the dielectric material refractive index and can lead to SPR based components presenting tunable properties.

In this paper, a way to obtain a tunable surface plasmon resonance with a grating coupling configuration is investigated. Diffraction gratings with surface plasmon resonances can exhibit broad or narrow spectral responses (from a few nanometers to a few tens of nanometers depending on the metal), light can be totally absorbed under suitable conditions [4,5] and such an effect can be useful in many different spectral filtering applications.

2. Principle of the device

The excitation of a surface plasmon with a diffraction grating relies upon the fulfilment of the following phase matching condition [2]:

* Corresponding author.
E-mail address: sebastien.massenot@enst-bretagne.fr (S. Massenot).

$$k_0\sqrt{\varepsilon_1}\sin\theta + m\frac{2\pi}{\Lambda} = k_{SP} \quad \text{with } k_{SP} = k_0\sqrt{\frac{\varepsilon_1\Re(\varepsilon_M)}{\varepsilon_1 + \Re(\varepsilon_M)}} \qquad (1)$$

where ε_1 is the permittivity of the incident medium, ε_M the permittivity of the metal, θ the incident angle, k_0 modulus of the wavevector in vacuum ($k_0 = 2\pi/\lambda$), Λ the grating period, m corresponds to the diffracted order use to excite the SPR and k_{SP} the propagation constant of the plasmon wave. The quantities involved in this relation are illustrated in Fig. 1.

From the phase matching relation (1), the only way to tune a surface plasmon resonance at fixed wavelength and without mechanical movement is to vary the permittivity of the incident medium. This can be made by using an electro-optical material of the polymer dispersed liquid crystals (PDLC) type. Such material is composed of liquid crystal (LC) domains (called usually droplets) dispersed in a polymer matrix as sketched in Fig. 2.

Such a material is obtained via the phase separation induced by the UV curing of a homogeneous mixture containing a monomer and a liquid crystal. By applying an electric field, the LC molecules can be oriented. Depending on the ratio between the LC droplet size and the operation wavelength, a phase change and/or scattering behaviour is obtained. If the droplet size is significantly smaller than the wavelength, the PDLC structure does not scatter and is essentially a varying index material [6]. In the present experimental work the near-infrared wavelength domain (1510–1580 nm) was chosen with a LC droplet size of the order of a few hundreds of nanometers, hence the name of "nano-PDLC" for the material.

This material possesses most of the advantages of liquid crystals (alignment of the molecules under the application of an electric field) but with an improved robustness of the liquid crystal phase due to the polymer network. Furthermore no alignment layers for the liquid crystal are needed. Refractive index variations of 0.02 are obtainable for electric field values of 10 V/μm. In this work, a nematic liquid crystal is used, switching times of the millisecond can be obtained for this device.

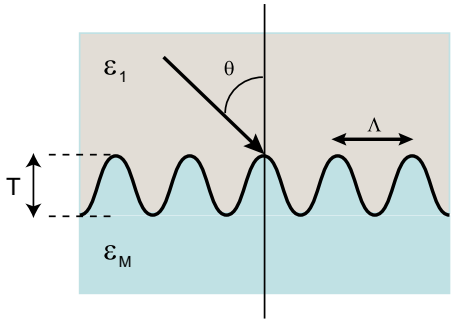

Fig. 1. Geometry and notations used in Eq. (1).

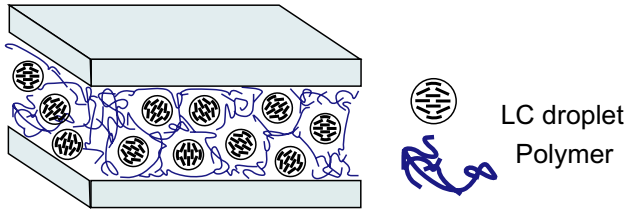

Fig. 2. Illustration of the PDLC structure.

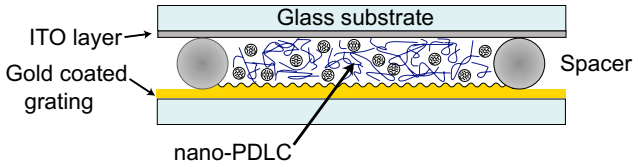

Fig. 3. Test structure.

The component used to test the principle is illustrated in Fig. 3. It is a conventional nano-PDLC cell where one electrode is the metallic grating allowing the excitation of a surface plasmon resonance (the other electrode is an ITO coated glass substrate). The cell is filled with a nano-PDLC material and spacers impose the cell thickness. An electric field applied transversally to the cell changes the average refractive index of the material and hence the surface plasmon resonance excitation condition.

Tunable SPRs using liquid crystals have been already reported in a RGB display application, but in a Kretschmann–Raether configuration (the SPR is excited via a prism) and with pure liquid crystals (alignment layers were required) [7].

In what follows, the design method of the device, the fabrication process and the most recent measurements will be described.

3. Design of the device

The modelling of the behaviour of the structure under study must account for the presence of a corrugated metallic part and describe the resonance of the TM polarization. To achieve this, the classical vector theory of Moharam et al. [8], which is currently used to model diffraction gratings, is not the most suitable because of the presence of metallic parts and the use of the TM polarization. More powerful methods were used, such as the C-method [9,10] and the differential method using the fast Fourier factorization and the scattering matrix algorithms [11]. Both methods use a Fourier expansion of the electromagnetic field but the C-method uses a coordinate transform which replaces the corrugation by a permittivity and permeability modulation at either side of a planar interface.

Considering first the metal grating alone, the position of the plasmon resonance is given by the phase matching relation (1). The value of the minimum of reflectivity is related with the modulation depth of the grating. An example is illustrated in Fig. 4 where the parameters of the grating have been optimized to attenuate a wavelength $\lambda = 1.55$ μm ($\Lambda = 1$ μm, $\varepsilon_1 = 1$, $\theta = 31.7°$ and $T = 36$ nm). In this case and in the following numerical simulations,

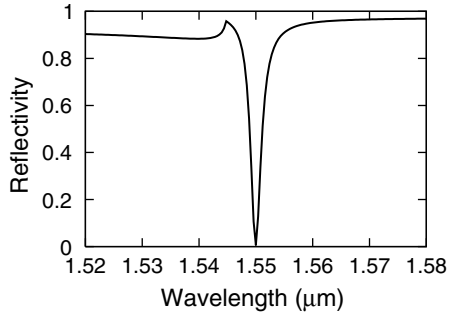

Fig. 4. Reflectivity of a gold grating with air cover calculated by means of the C method.

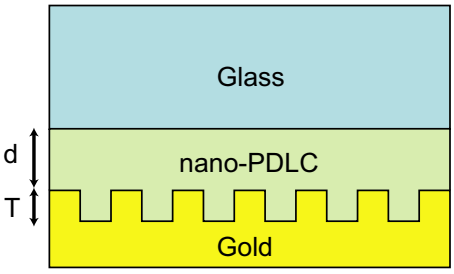

Fig. 5. Cell structure used for numerical simulations, $n_{\text{Glass}} = 1.519$ and $n_{\text{PDLC}} = 1.55$, $n_{\text{Gold}} = 0.559 + 9.81\jmath$, $\Lambda = 650$ nm, $T = 36$ nm and $\theta = 32.2°$.

the minus first order of the grating is retained to excite the surface plasmon.

The complete structure is then modelled by adding a cover layer and a semi-infinite superstate. For time computation reasons, simulations with a lamellar grating instead of a sinusoidal profile were performed. An illustration is shown in Fig. 5 where the top glass substrate is considered as semi-infinite.

The calculations were made by means of the differential method because of its suitability for an easy modelling of the propagation through homogeneous layers based on a grating. The results for different cell thicknesses and under TM polarized excitation are shown in Fig. 6.

In addition to the surface plasmon resonance, absorption peaks for wavelengths smaller than the plasmon wavelength are observed. The number of peaks increases with the cell thickness. These anomalies are due to the presence of the thin dielectric layer over the grating. They correspond to the excitation of guided modes of the structure [12,13] and they are coupled via the diffraction grating. The excitation condition of such guided modes is given by the relation (2):

$$k_0 n_{\text{Glass}} \sin\theta + m\frac{2\pi}{\Lambda} = \pm\beta \tag{2}$$

β is the propagation constant of the guided mode (the sign of the propagation constant corresponds either to a co-directional coupling or to a contra-directional coupling), θ is the incident angle in the glass cover, m the order of the grating used to excite the guided mode. In the following, the effective index n_{eff} of the mode will be used instead of the propagation constant ($\beta = k_0 n_{\text{eff}}$).

The excitation of guided modes can be checked by calculating the effective indices of the TM modes of the three-layer structure (gold substrate/nano-PDLC/glass cover) without the presence of the grating (see Fig. 7).

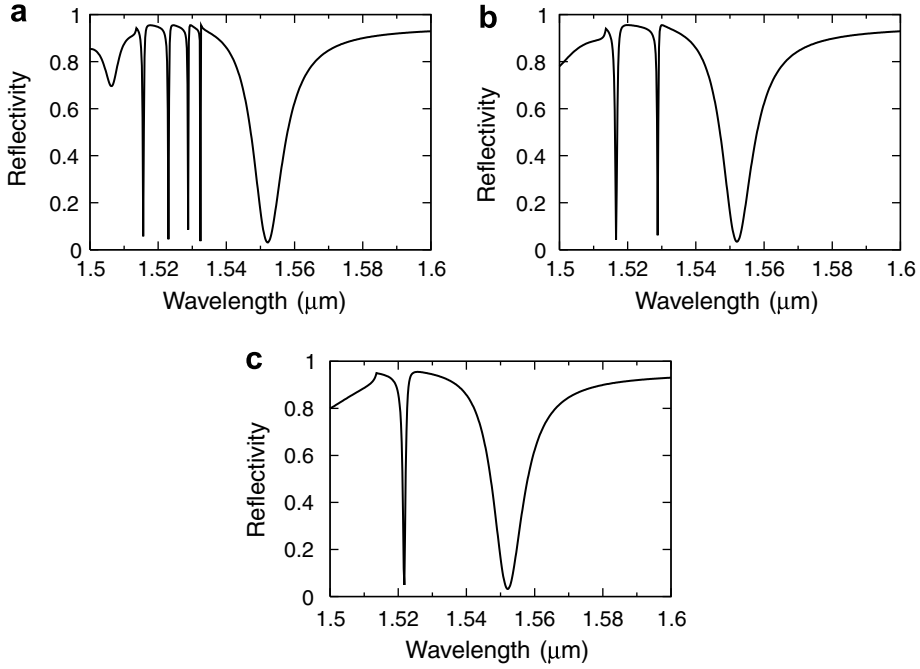

Fig. 6. Numerical simulations of the reflection of a cell structure under TM polarized excitation with different PDLC thicknesses: 10 μm (a), 5 μm (b) and 3 μm (c).

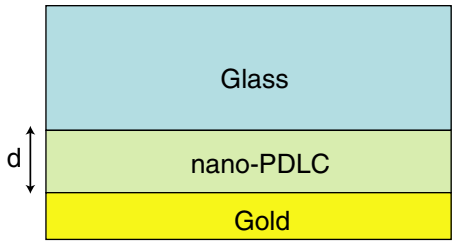

Fig. 7. Three-layer structure retained for the calculation of the guided modes. The parameters are the same as in Fig. 5.

Table 1
Effective indices values provided by solving Eqs. (2) and (3) for n_{eff}

d (μm)	Mode	λ_m (μm)	n_{eff}, Eq. (2)	n_{eff}, Eq. (3)
3	TM_1	1.5218	1.5318	$1.5306 + 2.964 \times 10^{-4}j$
5	TM_1	1.5288	1.5426	$1.5422 + 1.240 \times 10^{-4}j$
	TM_2	1.5166	1.5238	$1.5231 + 1.928 \times 10^{-4}j$
10	TM_1	1.5324	1.5481	$1.5480 + 0.208 \times 10^{-4}j$
	TM_2	1.5288	1.5426	$1.5423 + 0.625 \times 10^{-4}j$
	TM_3	1.5230	1.5336	$1.5333 + 0.980 \times 10^{-4}j$
	TM_4	1.5156	1.5223	$1.5219 + 1.091 \times 10^{-4}j$

Effective indices values are given by solving Eq. (3) for n_{eff}, it is the conventional dispersion relation of TM guided modes:

$$\arctan\left(\frac{\varepsilon_{PDLC}}{\varepsilon_{Glass}}\sqrt{\frac{n_{eff}^2-\varepsilon_{Glass}}{\varepsilon_{PDLC}-n_{eff}^2}}\right) + \arctan\left(\frac{\varepsilon_{PDLC}}{\varepsilon_{Gold}}\sqrt{\frac{n_{eff}^2-\varepsilon_{Gold}}{\varepsilon_{PDLC}-n_{eff}^2}}\right) + q\pi = \frac{2\pi d}{\lambda}\sqrt{\varepsilon_{PDLC}-n_{eff}^2} \quad (3)$$

q corresponds to the order number of the mode.

For each PDLC layer thickness in Fig. 6, the wavelength λ_m for which there is a strong absorption is determined and the corresponding effective indices is given by Eqs. (2) (grating coupling) and (3) (guided mode calculation). The case of a contra-directional coupling with the −1 order of the grating is considered. As the permittivity of gold is complex, solving Eq. (3) provides complex values for n_{eff}. Results for different guide thicknesses d are provided in Table 1.

Real parts of effective indices resulting from Eqs. (2) and (3) are in excellent accordance, which confirms that TM guided modes of the structure are excited indeed. Numerical differences are attributed to a perturbation of the guided mode by the grating corrugation.

4. Experiments

4.1. Fabrication and characterization of the metal grating

Metallic gratings were fabricated following the process described in Fig. 8: (a) a thin layer of Shipley S-1805 photoresist is deposited by spin-coating (4000 rpm) onto a glass substrate. The thickness necessary to excite a surface plasmon resonance, i.e. few tens of nanometers is obtained by an adequate dilution of the photoresist (a dilution of 3:10 of the resist has been retained). Then the holographic exposure of a sinusoidal grating pattern with the 488 nm line of an Ar+ ion laser is realized (5 min of exposition for an irradiance of 5.6 mW/cm^2); (b) The photoresist is developed in order to obtain a surface relief grating (with the developer microposit MF-303 diluted in deionised water at a ratio 1:14); (c) The grating is gold-coated using a sputtering technique. No adhesion layer is used between the resist corrugation and the gold film.

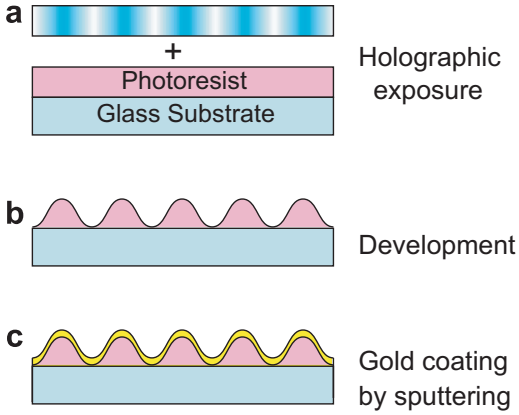

Fig. 8. Fabrication process of gold-coated gratings.

In Fig. 9a and b, SEM and AFM scans of uncoated gratings are shown (the period is here nearly 1.06 μm). AFM measurements of the grating profile give a modulation depth of 25 nm (which is a suitable value for exciting a surface plasmon resonance).

The gratings were optically characterized with a collimated near-infrared tunable laser (1510–1580 nm). The grating shown in Fig. 9 has been gold-coated and reflectivities measurements have been performed, results are shown in Fig. 10. A good agreement with the theory is observed. The fact that the resonance widths are not the same can be due to differences between refractive indices of massive and sputtered gold (see [14] for example).

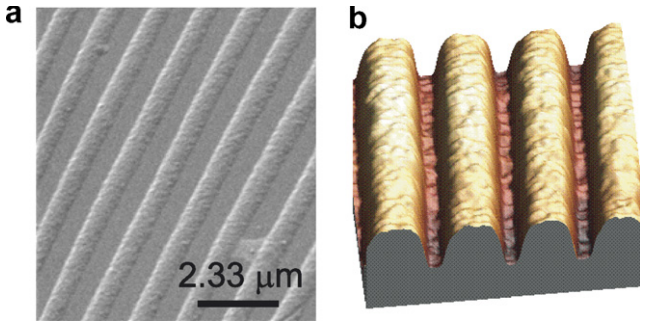

Fig. 9. Scanning electron micrograph (×12,900) (a) and AFM observations of the surface of the photoresist gratings (size of 4 μm × 4 μm) (b).

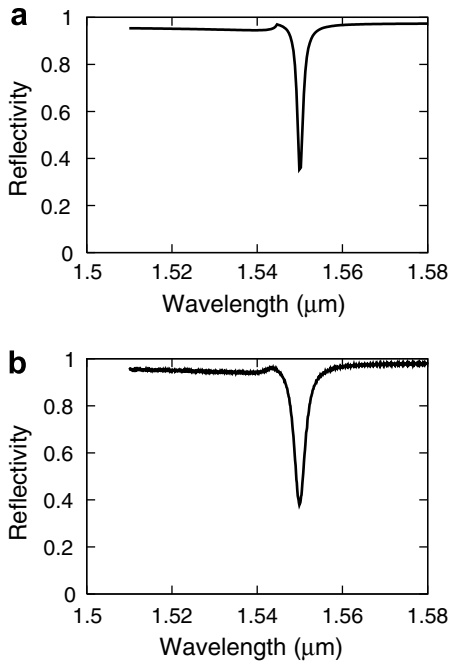

Fig. 10. Comparison between theoretical (a) and experimental (b) reflectivities for a sinusoidal gold grating of period $\Lambda = 1.06\,\mu m$, depth $T = 25$ nm and $\theta = 27.2°$.

This characterization phase was crucial in order to determine the different parameters of the grating fabrication process (irradiances and uniformity of the recording beams, exposure time, photoresist dilution, photoresist development time, and gold deposition parameters).

4.2. Study of the grating based nano-PDLC cell

A first set of nano-PDLC of different thicknesses d (10 μm, 5 μm and 3.5 μm) on a 700 nm period metallic grating was fabricated in order to check the behaviour predicted by the simulations. Cells were filled with a mixture NOA65 (Monomer from Norland)/BL036 (nematic liquid crystal from Merck) in a 50/50 ratio by weight. The mixture was cured for 10 min under a 170 mW/cm^2 UV exposure.

As predicted by the computer simulations, absorption peaks below the plasmon resonance due to the excitation of TM guided modes are observed, their number decreases with decreasing cell thickness as shown in Fig. 11. By comparing measurements for a 10 μm cell containing polymer only (Fig. 11a) and one containing the nano-PDLC (Fig. 11b), losses appear. They are due to light scattering by liquid crystal droplets (in addition, as a reflection grating is used, the incident light undergoes a double-pass in the material). Comparing to the theory (Fig. 6), a widening of the plasmon resonance is observed, notably for the 10 μm cell. This can be still attributed to losses of the PDLC layer. An illustration is shown in Fig. 12 where the reflectivity for a cell containing a lossy PDLC layer (Fig. 12b) is compared to loss less structure (Fig. 12a). An increase of the resonance width is observed.

Then, a 10 μm thick nano-PDLC cell with an ITO layer on the cover glass was realized in order to apply an electric field on the structure. Reflectivity measurements for varying electrical field are shown in Fig. 13. The resonance is displaced over a range of 20 nm by applying a voltage between 0 and 30 V which demonstrates the principle of

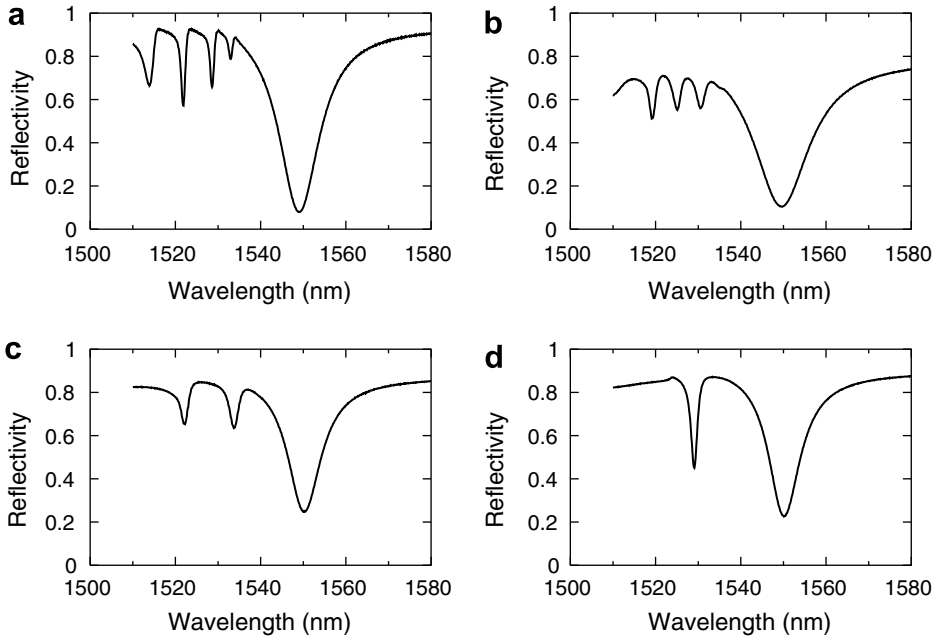

Fig. 11. Reflectivity measurements for nano-PDLC cells of different thicknesses: 10 μm filled with polymer only (a), 10 μm (b), 5 μm (c) and 3.5 μm (d).

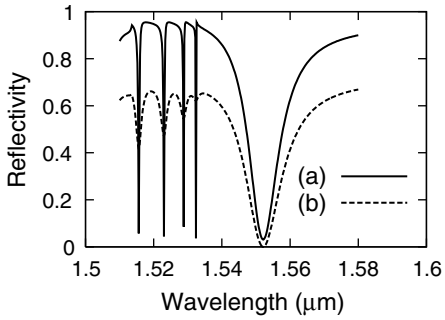

Fig. 12. Simulation results obtained for a 10 μm cell where $n_{PDLC} = 1.55$ (a) and $n_{PDLC} = 1.55 + 0.0015j$ (b), parameters are the same as in Fig. 6.

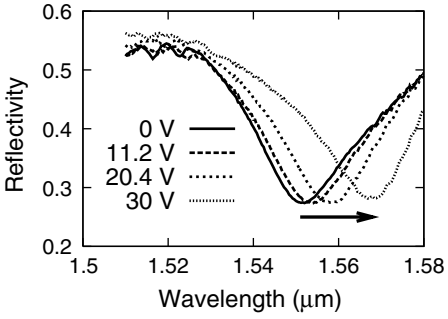

Fig. 13. Illustration of the displacement of the surface plasmon resonance with applied voltage.

the active element and that such element can be used as a tunable spectral filter.

This is not the optimum case for observing an ideal behaviour of the filter (presence of scattering losses and guided modes in the structure due to the high thickness of the cell) and further improvements are needed. The high thickness value has been first retained in order to avoid electrical contacts between the two electrodes (the gold layer over the grating being extremely fragile). Furthermore the grating depth value is not optimized to completely absorb the incident wave via the surface plasmon resonance.

5. Conclusion

The design and the fabrication of a tunable filter based on the surface plasmon phenomena by using a metallic diffraction grating and an electro-optical material has been presented. Due to the high number of parameters to be taken into account (obtaining a grating with the proper modulation depth, mastering the gold deposition process, the nano-PDLC cell assembly), the fabrication is not yet optimized but the principle of the displacement of the resonance has been demonstrated. These results and the theoretical behaviour lend us to expect that tunable filters with a range of several tens of nanometers under a voltage range of few tens of Volts can be built.

Such device could be applied to filter channels in optical telecommunication networks, mainly in metropolitan networks where the optical channels are spaced by tenth of nanometers (Coarse Wavelength Division Multiplexing Technology, CWDM). For a single channel, it could be used as a variable optical attenuator, the reflectivity of the centre wavelength of the channel being modified by an external electric field.

Acknowledgements

The authors acknowledge the contribution of Séverine Haesaert and Michel Gadonna from the CCLO laboratory (Centre Commun Lannionnais d'Optique, Lannion, France) who performed the SEM and AFM measurements.

References

[1] J. Homola, S.S. Yee, G. Gauglitz, Sensor Actuat B—Chem 54 (1999) 3.
[2] H. Raether, Surface Plasmons on Smooth and Rough Surfaces and on Gratings, Springer-Verlag, Berlin, 1988.
[3] W.L. Barnes, A. Dereux, T.W. Ebbesen, Nature 424 (2003) 824.
[4] M.C. Hutley, D. Maystre, Opt. Comm. 19 (1976) 431.
[5] L.B. Mashev, E.K. Popov, E.G. Loewen, Appl. Opt. 28 (1989) 2538.
[6] S. Matsumoto, Y. Sugiyama, S. Sakata, T. Hayashi, J. Intel. Mat. Syst. Struct. 10 (1999) 489.
[7] Y. Wang, Appl. Phys. Lett. 67 (1995) 2759.
[8] M.G. Moharam, D.A. Grann, E.B. Pommet, T.K. Gaylord, J. Opt. Soc. Am. A 12 (1995) 1068.
[9] J. Chandezon, D. Maystre, G. Raoult, J. Opt. (Paris) 11 (1980) 235.
[10] L. Li, J. Chandezon, G. Granet, J.-P. Plumey, Appl. Opt. 38 (1999) 304.
[11] M. Nevière, E. Popov, Light Propagation in Periodic MediaDifferential Theory and Design, M. Dekker Inc., New York, 2003.
[12] M. Nevière, D. Maystre, P. Vincent, J. Opt. (Paris) 8 (1977) 231.
[13] I. Pockrand, J. Phys. D: Appl. Phys. 9 (1976) 2423.
[14] L. Ward, The Optical Constants of Bulk Materials and Films, A. Hilger, Bristol, 1988.